# FLOW SIMULATIONS IN THE HUMAN CARDIOVASCULAR SYSTEM UNDER VARIABLE EXTERNAL CONDITIONS

**R. Adragna**[(a)]**, R.C. Cascaval**[(b)]**, M.P. D'Arienzo**[(c)]**, and R. Manzo**[(d)]

[(a),(b)]University of Colorado Colorado Springs, Department of Mathematics
[(c),(d)]Università degli Studi di Salerno, Dipartimento di Ingegneria dell'Informazione, Ingegneria Elettrica e Matematica Applicata

[(a)]radragna@uccs.edu, [(b)]radu@uccs.edu, [(c)]mdarienzo@unisa.it, [(d)]rmanzo@unisa.it

## ABSTRACT
In this paper we study the effects of variations in the external conditions (such as pressure changes due to motion in gravitational field) on the cardiovascular system. The goal is to understand how the flow and pressures propagate in the network in such variable conditions and which are the locations where the effects are significant. This is relevant to the auto regulation mechanism of the pressure and flow, designed to maintain the system in a homeostatic condition.

Keywords: vascular network, arterial pressure, blood flow, orthostatic change

## 1. INTRODUCTION
The primary role of the human cardiovascular system is to transport oxygen and nutrients to all the tissues of the body and to remove carbon dioxide and other harmful waste products of cell metabolism. From a physical point of view, the system consists of two synchronized pumps in parallel that propel a viscous liquid (the blood) through a network of flexible tubes. The heart provides energy to move blood through the circulatory system. It consists of four cavities: two ventricles and two atria, whose size varies during the cardiac cycle due to the activity of the heart muscle. The right heart pumps deoxygenated blood through the *pulmonary circulation* and the left heart pumps oxygen-rich blood through the *systemic circulation*. There are four valves, one at the exit of each heart cavity, which regulate blood flow in the heart and ensure bulk unidirectional motion through both pulmonary and systemic circulation (Formaggia, Lamponi and Veneziani 2006; Ottesen, Olfusen and Larsen 2004). The latter consists of a network of curved and branching vessels whose size decreases in the arteries, arterioles and capillaries and increases in the venules and veins. In particular, arteries distribute blood throughout the body and maintain blood pressure between heartbeats, arterioles transport blood to capillary beds, capillaries diffuse oxygen and nutrients to cells, and venules collect deoxygenated blood from capillaries and return it to the heart through veins. The topological pattern of the large systemic arteries is primarily a binary tree structure.

In this paper, we consider a simplified arterial network which contains the 55 largest arteries in the human body for the systemic circulation as presented in (Alaustrey, Parker and Sherwin 2012; Alaustrey 2006).

Numerically, we start with the standard hyperbolic system which models area $A = A(x,t)$ and velocity $U = U(x,t)$ in the spatial domain (Cascaval, D'Apice, D'Arienzo and Manzo 2015). At the junctions we use continuity conditions for the Bernoulli pressure and the continuity of the forward and backward characteristics for the hyperbolic system. The outflow is defined using peripheral resistance model. We solve the system with a discontinuous Galerkin scheme, using Gauss-Legendre method to approximate integrals and Newton method to find the solution of the Riemann problem at junctions. The entire system is simulated under variable external conditions such as variations in hydrostatic pressure due to posture changes, variations in respiratory patterns and variations in pressures due to exercise. The heart rate and peripheral resistance are used as controls for maintaining homeostatic conditions, which model the autoregulation mechanism. While an analytical treatment of the optimal control problem is out of reach due to the complexity of the system, numerical simulations of the entire system reveal the nature of the autoregulation mechanism under the considered variable external conditions. The novelty of this paper is to apply the numerical model of the entire 55-edge network to study the effects of the variable environment on the cardiovascular system performance, showing that the obtained results are consistent with the expected ones.

## 2. NUMERICAL MODEL
We consider the standard hyperbolic system which models area $A = A(x,t)$ and velocity $U = U(x,t)$ in the spatial

Proceedings of the European Modeling and Simulation Symposium, 2015
978-88-97999-57-7; Affenzeller, Bruzzone, Jiménez, Longo, Merkuryev, Zhang Eds.

228

domain $\Omega = [0, M]$ (Cascaval, D'Apice, D'Arienzo and Manzo 2015):

$$\frac{\partial A}{\partial t} + \frac{\partial (AU)}{\partial x} = 0,$$

$$\frac{\partial U}{\partial t} + U \frac{\partial U}{\partial x} + \frac{1}{\rho} \frac{\partial P}{\partial x} = f.$$

Here $f = f(A, U)$ is a friction force which models the viscosity of the blood, considered as a non-Newtonian fluid, $P = P(x, t)$ is the hydrodynamic pressure and $\rho$ is the density of the blood. For the pressure we choose the elastic model:

$$P = P_{ext} + \frac{\beta}{A_0}(\sqrt{A} - \sqrt{A_0}),$$

where $P_{ext}$ is the external pressure, $A_0$ is the cross-sectional area in unstressed conditions, $\beta = \frac{Eh_w}{1-\sigma^2}\sqrt{\pi}$, with $\sigma$ the Poisson ratio, usually taken to be $\sigma = \frac{1}{2}$, $E$ the Young modulus and $h_w$ the wall thickness.

Inflow conditions (at $x = 0$) are implemented using a valve model, which mimics the real behavior of the physiological system. The opening and closing of valve is determined by the pressure difference between the left ventricle ($P_{LV}$) and the aortic pressure. More specifically, the valve opens when

$$P(0, t) \leq P_{LV}(t),$$

in which case the pressure at the inflow gets prescribed

$$P(0, t) = P_{LV}(t),$$

and it closes when the velocity becomes negative, in which case the velocity at the inflow is prescribed to be zero:

$$U(0, t) = 0.$$

So:

$$U(0, t) = 0, \quad \text{if } P_{LV}(t) < P(0, t)$$
$$P(0, t) = P_{LV}(t), \quad \text{if } U(0, t) > 0$$

In the simulations, the left ventricular pressure is prescribed equal to

$$P_{LV}(t) = P_{ext} + 3.75 \frac{HR}{75} 10^{-4} \sin \frac{\pi t}{\tau},$$

with $HR$ representing the heart rate and $\tau$ the duration of the systole, taken to be a quarter of the heart beat ($\tau = 15/HR$). This model accounts for the fact that peak amplitude of the left ventricular pressure depends on the heart rate.

As terminal condition, we have used a model with *terminal reflection coefficient* $R_t$, see (Alastruey 2006), which is based on the assumption that $W_b$ is proportional to $W_f$:

$$W_b = -R_t W_f,$$

where $-1 \leq R_t \leq 1$ and $W_f$ and $W_b$ are the forward and backward characteristics, defined as:

$$W_{f,b} = u \pm (c(A) - c(A_0)), \quad c(A) = \sqrt{\frac{8\beta}{\rho A_0}} A^{1/4}.$$

Note that $R_t = 1$ corresponds to $u = 0$, which means the outflow is completely blocked, while $R_t = -1$ corresponds to $A = A_0$. For general values of $R_t \in [-1, 1]$ the boundary conditions is

$$U = \frac{1 - R_t}{1 + R_t} \sqrt{\frac{8\beta}{\rho A_0}} \left( A^{1/4} - A_0^{1/4} \right).$$

The spatial network considered in this paper is the standard 55-edge network representing the large arteries in a human. The labeling of the edges is taken from (Alastruey 2006).
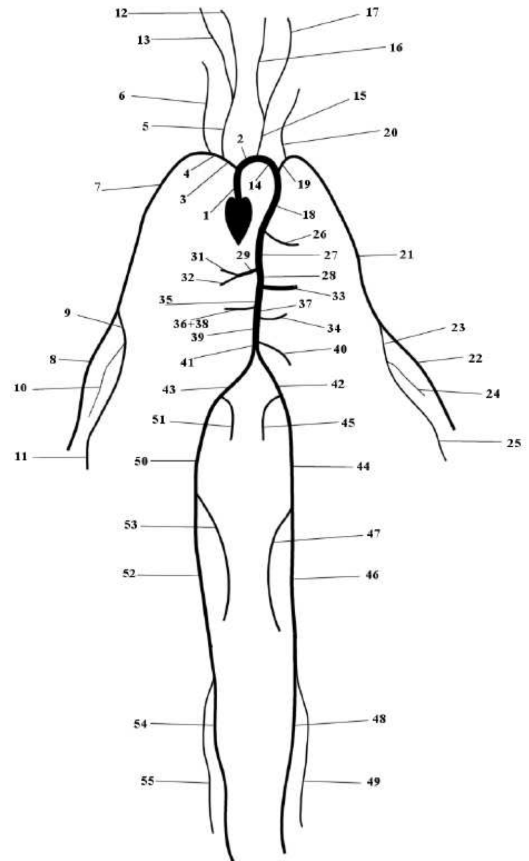


Figure 1: The spatial domain is a 55-edge network.

## 3. NUMERICAL SOLUTION

In order to find the numerical solution of the problem, we write the system in conservation form:

$$\frac{\partial \mathbf{U}}{\partial t} + \frac{\partial \mathbf{F}}{\partial x} = \mathbf{S}, \tag{1}$$

with

$$\mathbf{U} = \begin{bmatrix} A \\ U \end{bmatrix}, \mathbf{F}(\mathbf{U}) = \begin{bmatrix} AU \\ \frac{U^2}{2} + \frac{P}{\rho} \end{bmatrix}$$

Proceedings of the European Modeling and Simulation Symposium, 2015
978-88-97999-57-7; Affenzeller, Bruzzone, Jiménez, Longo, Merkuryev, Zhang Eds.

229

and $\mathbf{S}(\mathbf{U}) = \begin{bmatrix} 0 \\ \frac{1}{\rho}\left( \frac{f}{A} - \frac{\partial P}{\partial \beta}\frac{d\beta}{dx} - \frac{\partial P}{\partial A_0}\frac{dA_0}{dx} \right) \end{bmatrix}.$

We solve it using the discontinuous Galerkin scheme as described in (Cascaval, D'Apice, D'Arienzo and Manzo 2015).

We write the weak formulation of the problem, approximate $\mathbf{U}(x,t)$ with its discretized expansion $\mathbf{U}^\delta(x,t)$ and integrate twice by part, so we get:

$$\left(\frac{\partial \mathbf{U}^\delta}{\partial t}, \Phi^\delta\right)_\Omega + \left(\frac{\partial \mathbf{F}(\mathbf{U}^\delta)}{\partial x}, \Phi^\delta\right)_\Omega +$$
$$+ [(\mathbf{F}^u - \mathbf{F}(\mathbf{U}^\delta)) \cdot \Phi^\delta]_0^M = (\mathbf{S}(\mathbf{U}^\delta), \Phi^\delta)_\Omega. \quad (2)$$

To simplify the method, we have mapped each elemental region onto the standard element $\Omega_{st} = \{\xi \in \mathbb{R} : -1 \le \xi \le 1\}$. This mapping is defined as

$$\chi(\xi) = M\frac{1+\xi}{2}, \qquad \xi \in \Omega_{st},$$

and its inverse is given by

$$\xi = \chi^{-1}(x) = 2\frac{x}{M} - 1, \qquad x \in \Omega.$$

We selected as expansion basis the Legendre polynomials $L_k(\xi)$, with $k$ the polynomial order, because they are orthogonal with respect to the product inner product of $L^2$. In this way, the solution is expanded on $\Omega$ as

$$\mathbf{U}^\delta(\chi(\xi),t) = \sum_{k=0}^{K} L_k(\xi)\widehat{\mathbf{U}^k}(t), \quad (3)$$

with $\widehat{\mathbf{U}^k}(t)$ the time-varying coefficients of the expansion. We have chosen Legendre points (which are the zeros of Legendre polynomials) as collocation points.
Replacing (3) in (2) and letting $\Phi^\delta = \mathbf{U}^\delta$, we obtain the following system of $2(K+1)$ differential equations to be solved:

$$\frac{d\widehat{U_i^k}}{dt} = \mathcal{F}_i^k(\mathbf{U}^\delta), \ k = 0, ..., K, \ i = 1, 2,$$

where $\widehat{U_i^k}, i = 1, 2$, are each of the two components of $\widehat{\mathbf{U}^k}(t)$ and

$$\mathcal{F}_i^k(\mathbf{U}^\delta) = -\left(\frac{\partial F_i}{\partial x}, L_k\right)_\Omega +$$
$$-\frac{2}{M}[(F_i^u - F_i(\mathbf{U}^\delta))(L_k \circ \xi)]_0^M + (S_i(\mathbf{U}^\delta), L_k)_\Omega.$$

The method is completed with a second-order Adams-Bashforth time-integration scheme:

$$\left(\widehat{U_i^k}\right)^{n+1} = \left(\widehat{U_i^k}\right)^n + \frac{3\Delta t}{2}\mathcal{F}\left((\mathbf{U}^\delta)^n\right) +$$
$$-\frac{\Delta t}{2}\mathcal{F}\left((\mathbf{U}^\delta)^{n-1}\right),$$
$$k = 0, ..., K, \quad i = 1, 2,$$

in which $\Delta t$ is the time step and $n$ the number of every time step. To calculate the integrals we use a Gauss quadrature formula of order $q \ge K + 1$.

The upwinded fluxes $\mathbf{F}^u$ are computed solving a Riemann problem that takes into account the characteristic information moving away. At a time $t$, each interface separates two constant states, $(A_L, U_L)$ and $(A_R, U_R)$, and we need to determine the two upwinded states, $(A_L^u, U_L^u)$ and $(A_R^u, U_R^u)$, originated on each side of interface at time $t + \Delta t$. To do this, the following equations are required:

$$\begin{aligned} W_f(A_L, U_L) &= W_f(A_L^u, U_L^u), \\ W_b(A_R, U_R) &= W_b(A_R^u, U_R^u), \\ A_L^u U_L^u &= A_R^u U_R^u, \\ \rho\frac{(U_L^u)^2}{2} + P(A_L^u) &= \rho\frac{(U_R^u)^2}{2} + P(A_R^u). \end{aligned} \quad (4)$$

The first two equations come from the assumption that the flow between two initial states is inviscid, and the forward characteristic information, $W_f$, and the backward characteristic information, $W_b$.

## 4. SIMULATION RESULTS

In this section we describe simulation results obtained by considering the 55-edge network presented above. We have taken input data, such as length, radius, terminal coefficient and $\beta$ for each edge from (Formaggia, Lamponi, Tuveri and Veneziani 2006).

We perform a 4-second simulation of the entire 55-edge network with variable external pressure (to account for respiration). The timing of the heart beat and respiratory cycle are taken from real data collected on a healthy individual in the physiology lab at University of Colorado (see Figure 2).
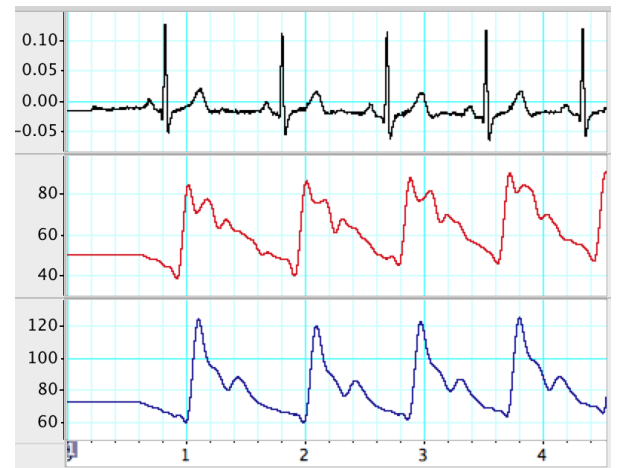


Figure 2: Real data for EKG (black), middle cerebral artery flow velocity in cm/s (red) and arterial blood pressure in mmHg (blue).

Since pressure and flow data are collected only at two sites in the network (radial artery for pressure and middle cerebral artery for flow), the simulation accomplishes to describe the dynamics in all other edges, hence completing the *picture* of the entire network. While the focus was

Proceedings of the European Modeling and Simulation Symposium, 2015
978-88-97999-57-7; Affenzeller, Bruzzone, Jiménez, Longo, Merkuryev, Zhang Eds.

230

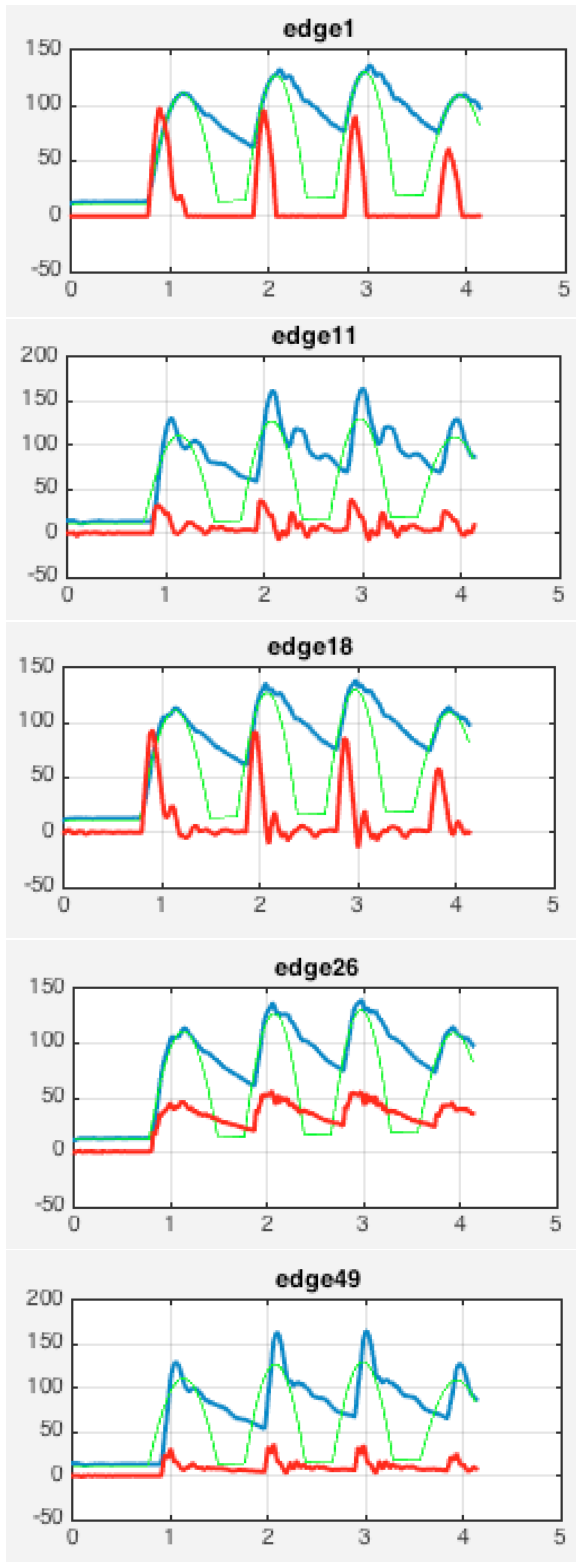on developing a working model, no data fitting was done for pressure and flow.



Figure 3: Simulated data in edge 1 (ascending aorta), 11 (right ulnar artery), 18 (thoracic aorta), 26 (intercostal artery) and 49 (anterior tibial artery). Red line is the flow velocity (cm/s), blue is the arterial pressure (mmHg) and green line is the left ventricular pressure.

In the root edge (edge 1) we see the valve in action: the valve is closed hence zero flow goes through it when the left ventricular pressure is lower than the aortic pressure; the valve opens when the left ventricular pressure exceeds the aortic pressure. The timing of the opening of the valve is important, since it determines the total amount of cardiac output. At the other extreme, in edge 49, the pulsatility of the flow is minimal, but still the influence of the respiratory cycle is evident.

There are several noticeable features in this simulation results. The edges depicted in Figure 3 are chosen to illustrate the various aspects of the dynamics. Firstly, the slow variation of the left ventricular pressure (e.g. due to respiration) causes visible variation in the systolic pressure. Secondly, the characteristics of the pressure and flow dynamics is significantly different across the network: in some parts of the network there is small amount of backflow (e.g. edge 11, 18) while in others there is no backflow, (e.g. edge 26). In fact backflow is significant in edges 4, 7, 19 and 21 (only edge 4 is depicted below). Backflow is known to be physiological.
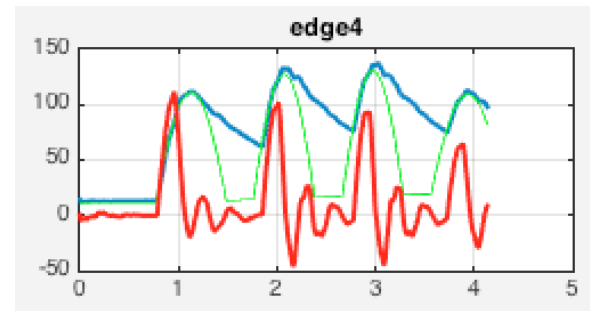


Figure 4: Simulated data in edge 4 (subclavian artery). For the color coding we refer to Figure 3.

For the remaining of this section, we apply the numerical model to a different scenario, that of a tilt test: The body is initially on a horizontal bed, with no orthostatic pressure differences throughout the network. After 2 seconds, a tilt of the table is performed, in such a fashion that the level of the heart remains the same. This means that the majority of the body is sent downward with the exception of the head and shoulders, creating an added orthostatic pressure value in most parts of the network.

Mathematically, this translates to a modification of the external pressure in our working model, to account for the gravitational effect (orthostatic pressure) as it appears during the tilt table test (see e.g. Olufsen, Ottesen, Tran, Ellwein, Lipsitz, and Novak 2005).

$$P_{ext} = P_{ext}(t) = \rho g h(t) = \rho g \Delta h \sin \alpha t$$

where $\alpha = \frac{\pi}{2}$ is the angular velocity, chosen in such a way that after 1 second the tilt table is in upright position, $g = 9.8 m/s^2$ is the gravitational constant. $\Delta h$ is elevation change between the middle of the edge and the heart when the person is upright. $\Delta h$ can be positive (if

the edge is below the heart) or negative (for edges that lie above the heart level.) Depending on what the center of the tilt is, $\Delta h$ values would have more negative values.

Next we display the simulated data for the flow velocity for both horizontal position and during and after tilt, choosing the same edges as for pressure.
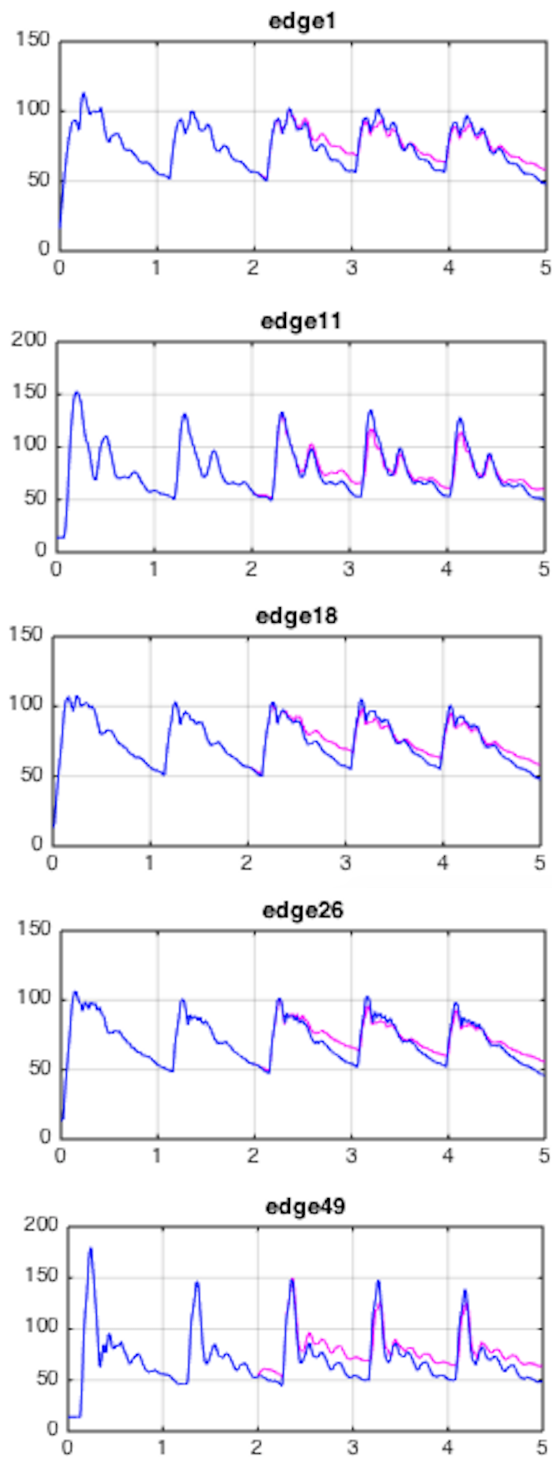


Figure 5: Comparison between the simulated pressure data (in mmHg) in normal conditions (blue) and in presence of the tilt (magenta) in edge 1 (ascending aorta), 11 (right ulnar artery), 18 (thoracic aorta), 26 (intercostal artery) and 49 (anterior tibial artery)
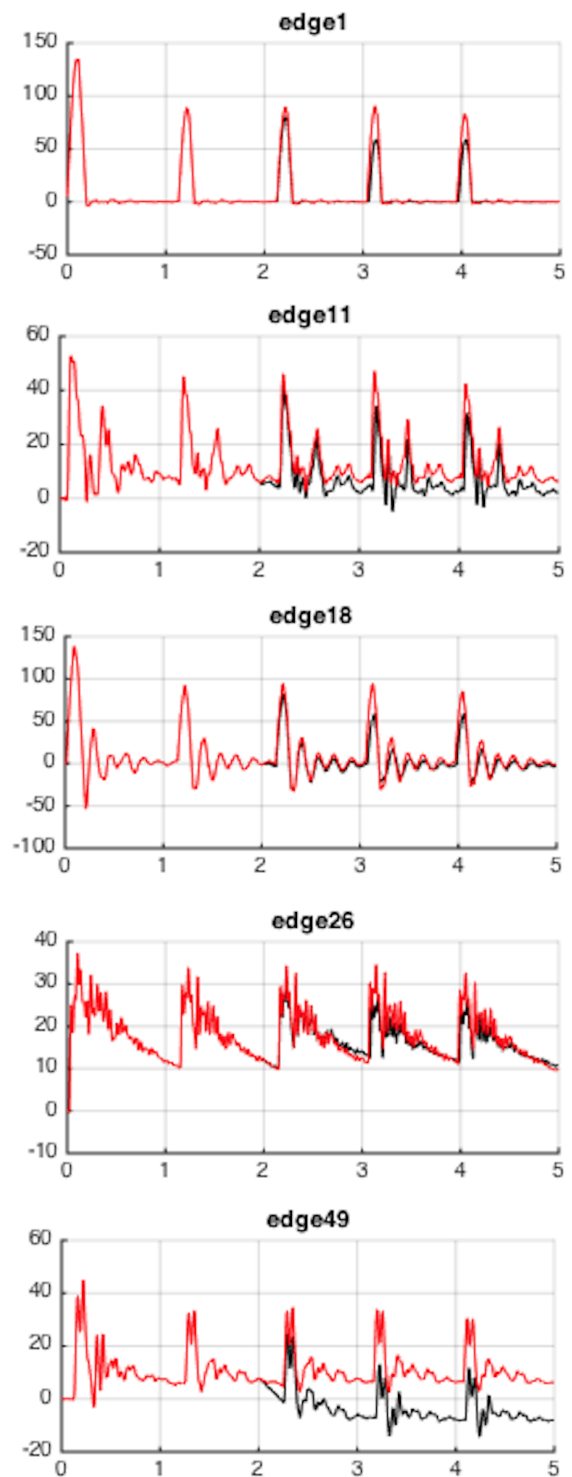


Figure 6: Comparison between the simulated flow velocity data (in cm/s) in normal conditions (blue) and in presence of the tilt (magenta) - same edges chosen for visualization as for pressure on the left

Proceedings of the European Modeling and Simulation Symposium, 2015
978-88-97999-57-7; Affenzeller, Bruzzone, Jiménez, Longo, Merkuryev, Zhang Eds.

232

The tilt is performed for 1 second (seconds 2-3 after the beginning of the simulations), time in which the table is raised from horizontal to vertical positions. Then the table is left at that level. We note that several edges come with negative external pressure. Nevertheless, the simulated data shows an increase of diastolic pressure throughout the board. At the same time, the picture with the flow pattern is much more diverse, several edges exhibiting a drop in flow velocity. The simulations are done without changing the Heart Rate calculations, for clarity of the comparison. In reality there is a response of the HR to the change in pressures (baroreceptor control), which would further alter the flow pattern. But even in absence of this complexity, we see that the systolic pressure is decreased immediately after the end of the tilt period, while the diastolic pressure is increased.

## 5. CONCLUSIONS

A numerical model has been developed here to simulate variable external conditions and their effect on the cardiovascular system, as presented in certain realistic physiological situations. The model includes a valve at the inflow, which accounts for change in the systolic pressure, while the variability of the diastolic pressure is due primarily to the external conditions. The focus has been on comparing the dynamics in various parts of the network in presence and absence of the changes. A real control of the heart rate and peripheral resistance is not present in our paper, but it will be reported elsewhere.

## REFERENCES

Alastruey, J., Parker, K.H., Sherwin, S.J., 2012. Arterial pulse wave haemodynamics. BHR Group's 11th International Conference on Pressure Surges, Lisbon, Portugal, 401–442.

Alastruey, J., 2006. Numerical Modelling of Pulse Wave Propagation in the Cardiovascular System: Development, Validation and Clinical Applications, PhD Thesis, Imperial College London.

Cascaval R.C., D'Apice C., D'Arienzo M.P., Manzo R., 2015. Flow Optimization in Vascular Networks, submitted to Math Biosci Eng.

Formaggia, L., Lamponi, D., Tuveri, M., Veneziani, A., 2006. Numerical modeling of 1D arterial networks coupled with a lumped parameters description of the heart. Comp. Meth. Biomech. Biomed. Eng., 9, 273–288.

Ottesen, J.T., Olufsen, M.S., Larsen, J.K., 2004. Applied Mathematical Models in Human Physiology, SIAM.

Olufsen, M.S., Ottesen, J.T., Tran, H.T., Ellwein, L.M., Lipsitz, L.A. and Novak, V., 2005. Blood pressure and blood flow variation during postural change from sitting to standing: model development and validation, J Appl Physiol 99: 1523–1537.

## AUTHORS BIOGRAPHY

**Reece Adragna** Reece Adragna is a graduate student in the Department of Mathematics at University of Colorado Colorado Springs (UCCS). His e-mail address is radragna@uccs.edu.

**Radu C. Cascaval** Dr. Cascaval is Associate Professor of Mathematics at University of Colorado Colorado Springs. His main research interests are in mathematical modeling in physiology. He has had several collaborations with exercise physiology faculty at University of Colorado and has recently won a grant from the BioFrontiers Institute at University of Colorado. His e-mail address is radu@uccs.edu.

**Maria Pia D'Arienzo** Maria Pia D'Arienzo was born in 1989 in Salerno. She graduated in Mathematics in 2012, at Univesity of Salerno, Italy. Now she is a PhD student in Mathemathics at University of Salerno. Her main research area is in fluid-dynamic models in physiology. Her e-mail address is mdarienzo@unisa.it.

**Rosanna Manzo** Rosanna Manzo is a researcher in Mathematical Analysis at the Department of Information Engineering and Electrical Engineering and Applied Mathematics of the University of Salerno, Italy. She received PhD in Information Engineering from University of Salerno. Her research areas include fluid - dynamic models for traffic flows on road, telecommunication and supply networks, optimal control and queueing theory. Her e-mail address is rmanzo@unisa.it.

Proceedings of the European Modeling and Simulation Symposium, 2015
978-88-97999-57-7; Affenzeller, Bruzzone, Jiménez, Longo, Merkuryev, Zhang Eds.

233